Nanoscale Horizons

ROYAL SOCIETY OF CHEMISTRY

REVIEW

View Article Online
View Journal | View Issue

Cite this: *Nanoscale Horiz.*, 2021, **6**, 766

Lanthanide upconversion and downshifting luminescence for biomolecules detection

Guotao Sun,[a] Yao Xie,[b] Lining Sun *[ab] and Hongjie Zhang *[c]

Received 31st May 2021,
Accepted 29th July 2021

DOI: 10.1039/d1nh00299f

rsc.li/nanoscale-horizons

Biomolecules play critical roles in biological activities and are closely related to various disease conditions. The reliable, selective and sensitive detection of biomolecules holds much promise for specific and rapid biosensing. In recent years, luminescent lanthanide probes have been widely used for monitoring the activity of biomolecules owing to their long luminescence lifetimes and line-like emission which allow time-resolved and ratiometric analyses. In this review article, we concentrate on recent advances in the detection of biomolecule activities based on lanthanide luminescent systems, including upconversion luminescent nanoparticles, lanthanide–metal organic frameworks, and lanthanide organic complexes. We also introduce the latest remarkable accomplishments of lanthanide probes in the design principles and sensing mechanisms, as well as the forthcoming challenges and perspectives for practical achievements.

1. Introduction

Lanthanide ions as luminescent probes have drawn much attention due to their unique properties from f–f electron transitions in the $[Xe]4f^n5s^25p^6$ (n = 1–14) electronic conformation.[1–6] These special spectroscopic properties, including long luminescence lifetimes, resistance to photobleaching, large Stokes or anti-Stokes shifts, and narrow emission bands, are suitable for analytes detection. Long luminescence lifetimes make time-resolution technology possible, which can reduce the influence of background luminescence and drastically improve the signal-to-noise ratio. Resistance to photobleaching offers long-term stability of luminescence *in vitro* and *in vivo*, enabling reliable and accurate results. Large Stokes shifts eliminate the overlap between absorption and emission spectra and avoid the reduction of fluorescence efficiency caused by energy transfer. The narrow emission band caused by 4f orbitals shielded by the 5s and 5p orbitals can improve the detection sensitivity toward analytes. These unique properties of the lanthanides provide a luminescent toolbox for the detection of biomolecules, anions, metal ions, pH values, temperature, drugs, gases, and reactive oxygen species, and so on.[7–17]

The luminescent mechanisms of lanthanide ions can be divided into two categories, upconversion luminescence and traditional downshifting luminescence (Fig. 1). Lanthanide upconversion luminescence is an anti-Stokes shift process

[a] *School of Materials Science and Engineering, Shanghai University, Shanghai 200444, China. E-mail: lnsun@shu.edu.cn*
[b] *Research Center of Nano Science and Technology, College of Sciences, Shanghai University, Shanghai 200444, China*
[c] *State Key Laboratory of Rare Earth Resource Utilization, Changchun Institute of Applied Chemistry, Chinese Academy of Sciences, Changchun 130022, China. E-mail: hongjie@ciac.ac.cn*

Guotao Sun

Guotao Sun received his BSc in Functional Materials from Qingdao Agricultural University in 2016. Then he received his MSc degree in Materials Science supervised by Prof. Jianguo Tang from Qingdao University in 2019. Now he is pursuing his PhD under Prof. Lining Sun at Shanghai University. His research focuses on lanthanide upconversion and down-shifting luminescence and their applications in biosensing.

Yao Xie

Yao Xie received his BSc in Chemistry from the Civil Aviation University of China in 2019. Now he is pursuing his PhD supervised by Prof. Lining Sun at Shanghai University. His research focuses on lanthanide-doped nanoparticles and their multi-functional applications.

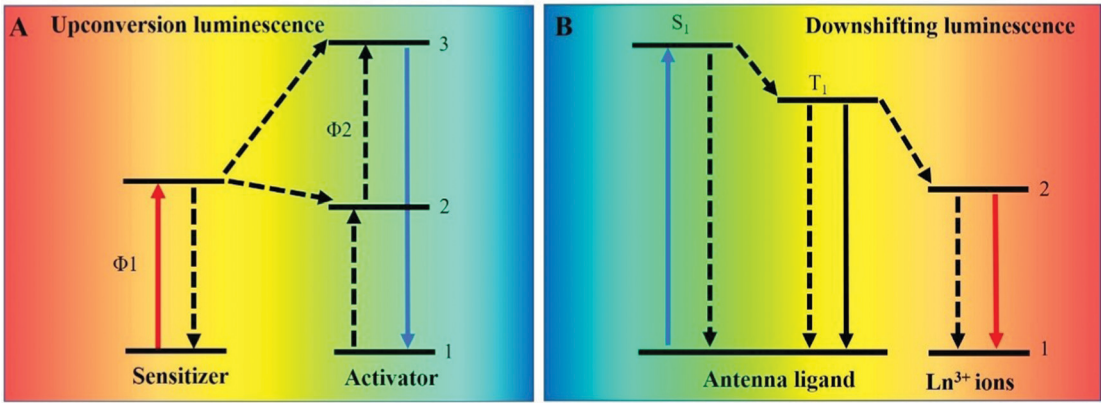

Fig. 1 Schematic illustrations of lanthanide upconversion (A) and downshifting (B) luminescence. 1 represents the ground state, and 2 and 3 represent the excited states.

where lanthanide ions absorb lower energy photons and emit higher energy photons, while downshifting luminescence is a Stokes shift process in which higher energy excitation light is converted into lower energy emission light. For the lanthanide upconversion process, upconversion nanoparticles (UCNPs) are the typical representation. For the downshifting process, lanthanide-metal organic frameworks (Ln-MOFs) and lanthanide organic complexes which consist of lanthanide ions as luminescent centers and organic molecules as antenna ligands are the primary subjects of study.

Recently, with the development of biomedicine applications, biomolecules associated with biological activities and many diseases have attracted increasing interest in the sensing field.[18–24] The stable, selective and sensitive detection of biomolecules by prospective luminescent probes holds much promise for specific and rapid biosensing. Up to now, a variety of successful biomolecule detection approaches and techniques have been developed. However, the disadvantages for implementation such as cost, reproducibility, mobility, and efficiency often lead to hard decisions under biological conditions. Recently, luminescent probes have been widely applied for biomolecule detection due to their unique optical properties. Traditional sensing techniques such as high performance liquid chromatography (HPLC) and liquid chromatography-mass chromatography usually cost much time and money and require a laboratorial environment to operate, while lanthanide luminescent probes are often cheap and can be applied in a wide range of situations owing to their easy fabrication and portability. Lanthanide probes allow the identification of a variety of analytes and factors according to the changes in wavelength, emission intensity, luminescence lifetimes or polarization.[8,25–27]

Lining Sun

Professor Lining Sun received her PhD degree in Chemistry from Changchun Institute of Applied Chemistry, Chinese Academy of Sciences (Supervisor: Prof. Hongjie Zhang). Then, from March 2008 to September 2009, she was an Alexander-von-Humboldt Research Fellow in the University of Regensburg, Germany, working with Prof. Otto S. Wolfbeis. In September 2009 she joined Shanghai University as an Associate Professor. Since March 2016, she has worked as a Full Professor of Chemistry and Materials. Her research interests mainly focus on lanthanide down-shifting luminescent materials and rare-earth doped upconversion luminescent nanomaterials for sensing, bioimaging, and therapy applications.

Hongjie Zhang

Professor Hongjie Zhang received his BSc from Peking University in 1978. He then worked as a research assistant in Changchun Institute of Applied Chemistry, Chinese Academy of Sciences (CAS), where he received his MSc in Inorganic Chemistry in 1985. Then, he worked as an Assistant Professor at Changchun Institute of Applied Chemistry, CAS, from 1985 to 1989. He then studied at the Université de Bordeaux I, Laboratoire de Chimie du Solide de CNRS (France), where he received his PhD degree in Solid State Chemistry and Material Sciences in 1993. He joined Changchun Institute of Applied Chemistry, CAS, as a Full Professor in 1994. He is an elected Member of Chinese Academy of Sciences (2013) and a Fellow of the Academy of Sciences for the Developing World (TWAS, 2014). His current research interests focus on rare earth luminescent materials, electroluminescent devices, functional nanomaterials, and rare earth magnesium alloys, and exploring their applications.

Several remarkable review articles have been published to emphasize the potential of lanthanide-related materials for bioimaging and biomedicine achievements.[4,28–30] In this review, we will concentrate on the literature of the past few years covering the recent advances of lanthanide-based systems for the detection of biomolecules. We begin by surveying the recent advances in the designed UCNPs to detect biomolecules, including amino acids, proteins, tumor biomarkers, nucleic acids, and so on. Next, we give a careful overview of the detection principles of Ln-MOFs and lanthanide complexes for biomolecules and discuss their sensing mechanisms and detection formats. We finish the review by assessing current challenges and presenting the prospects of lanthanide-based luminescent probes for fundamental studies and biomolecule detection.

2. Lanthanide upconversion luminescence for biomolecules detection

Lanthanide-doped UCNPs make use of the absorption of multiple photons *via* the long luminescence lifetimes and line-like energy levels of lanthanide ions.[31] The dopants of trivalent lanthanide ions as active centers convert two or more low-energy photons (NIR light) into shorter wavelength emissions (shorter NIR, visible, or UV light). The UCNPs have several attributes that make them suitable for biomolecule detection. For sensing applications, the virtually zero autofluorescence background in biological solutions can improve the signal-to-noise ratio; narrow emission bandwidths afford multiplexed detection; large anti-Stokes shifts enable researchers to distinguish the fluorescence from the excitation wavelength easily; and high resistance to photobleaching makes the detection more reliable in long-term testing.

The design of most UCNP-based biomolecule detection systems reported up to now is usually dependent on the Förster resonance energy transfer (FRET) effect in which the detection results rely on the luminescence switch off/on or lifetime variations. FRET is a mechanism which describes the energy transfer process when the emission spectrum of an energy donor and the excitation spectrum of an energy acceptor overlap. The energy transfer process usually occurs when the donor chromophore and acceptor chromophore are in close proximity.[32] So, the efficiency of the energy transfer is extremely sensitive to small changes in distance.[33,34] During the FRET process, UCNPs usually serve as energy donors. By making use of surface decorating strategies, a series of energy acceptors, like metal nanoparticles and organic dyes, have been modified onto the surfaces of UCNPs for sensing various analytes. In this part, we will review the recent achievements of designed UCNPs to perform high performance detection toward biomolecules.

2.1 Amino acids and protein detection

Amino acids are one of the many classes of biologically active macromolecules that construct biological organisms, and they are the basic materials for constructing cells and repairing tissues. In order to detect the content of various amino acids in the human body, a variety of sensors based on UCNPs have been developed. For example, Li *et al.* used the hemicyanine dye to modify UCNPs and developed a ratiometric fluorescent Arg-nanoprobe based on luminescence resonance energy transfer (LRET).[35] The nanoprobe can quantitatively detect arginine in a certain concentration range (528–1250 μM) and the limit of detection is determined to be 15.6 μM. In addition, some nanoprobes based on the emission–reabsorption (secondary internal filtering effect) process have also been studied. Su *et al.* constructed an up-conversion fluorescent sensor (UCNP@SiO_2-SP) that can specifically detect histidine.[36] When histidine is mixed with UCNP@SiO_2-SP, histidine can specifically bind to spiropyran and cause the isomerization of spiropyran. The luminescence of the sensor overlaps with the absorption of the isomerized spiropyran, which causes fluorescence quenching, leading to the sensing of histidine.

Amino acid derivatives are substances formed by the combination of amino acids through a series of reactions. Various amino acid derivatives play important roles in the human body, so a series of nanosensors based on amino acid derivatives have also been developed. Glutathione (GSH) is an important type of amino acid derivative. Zheng and colleagues constructed a nanoprobe that can simultaneously detect the GSH/H_2O_2 ratio.[37] As shown in Fig. 2A, the UCNPs are simultaneously linked to TCG (GSH sensitive dye) and BCH (H_2O_2 sensitive dye). The ratios of the upconversion luminescence intensities at 540 and 650 nm to that at 800 nm are

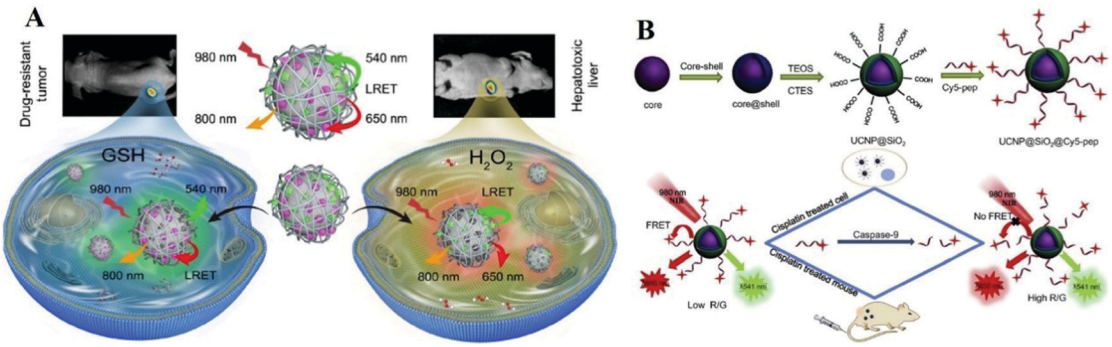

Fig. 2 (A) Schematic diagram of an upconversion nanoprobe that can simultaneously monitor GHS and H_2O_2 *in vivo*.[37] Copyright 2019, Springer Nature. (B) Schematic diagram of a nanosensor that can be used to detect caspase-9 activity *in vivo* and *in vitro*.[40] Copyright 2019, Elsevier.

used as detection signals, respectively. Liu's group proposed a new strategy to use organic dyes as targets to adjust the sensitization switch to prepare upconversion nanoprobes to detect intracellular GSH.[38] The organic dye acts as both a target's identification unit and a potential antenna. Before reacting with the target, the dye is non-emissive and will not be sensitized. After reacting with GSH, the dye will emit light strongly and cause upconversion luminescence sensitization through the nonradiative energy transfer process.

Amino acids are dehydrated and condensed into proteins, which are important biological macromolecules that compose all cells and tissues of the human body. Many upconversion nanoprobes for detecting proteins and enzymes have been successfully investigated. For example, Wang's group developed a new strategy to prepare intelligent upconversion fluorescent materials for highly specific enrichment and sensing of glycoproteins.[39] Song's group successfully constructed a FRET sensing system based on peptide-functionalized UCNPs,[40] which can detect caspase-9 *in vivo* and *in vitro*. As shown in Fig. 2B, the cleavage of Cy5 fragments on the surfaces of the UCNPs by caspase 9 leads to the restoration of red upconversion fluorescence. Higher caspase-9 activity will cause stronger recovery of the red emission. The signal intensity ratio of the red emission to green emission of the UCNPs is linearly related to the caspase-9 activity. You *et al.* also utilized the FRET effect to develop a new type of nanoprobe based on UCNPs conjugated with phycocyanin to detect the fluctuation of myeloperoxidase.[41] Phycocyanin is attached onto the surfaces of the UCNPs through amidation reaction, and the luminescence of the UCNPs is quenched by energy transfer from phycocyanin. The luminescence of the nanoprobe will be restored after phycocyanin specifically recognizes the myeloperoxidase. Using the same sensing strategy, Zhang's group designed sandwich-structured UCNPs ($NaYF_4$:Yb/Er@$NaErF_4$@$NaYF_4$), which can serve as a nanoprobe for the detection of alkaline phosphatase.[42] The UCNPs act as an energy donor in this system, and the complex, composed of ferric ions and sulfosalicylic acid, acts as an energy acceptor. In the presence of phosphate, the ferric ions were separated from the complex and coordinated with phosphate ions, resulting in an impediment to the energy transfer and the recovery of luminescence.

2.2 Tumor biomarkers detection

Cancer, as one of the most life-threatening diseases, has caused huge numbers of deaths globally despite a lot of research efforts, and is generally acknowledged to result mainly from tumor metastasis and late diagnosis.[43–45] The presence of tumor biomarkers usually accompanies the formation of tumors.[46,47] Many strategies aiming for early diagnosis of tumors have concentrated on discovering tumor biomarkers.[48–51] UCNPs as an important lanthanide probe have been also utilized for monitoring tumor biomarkers.

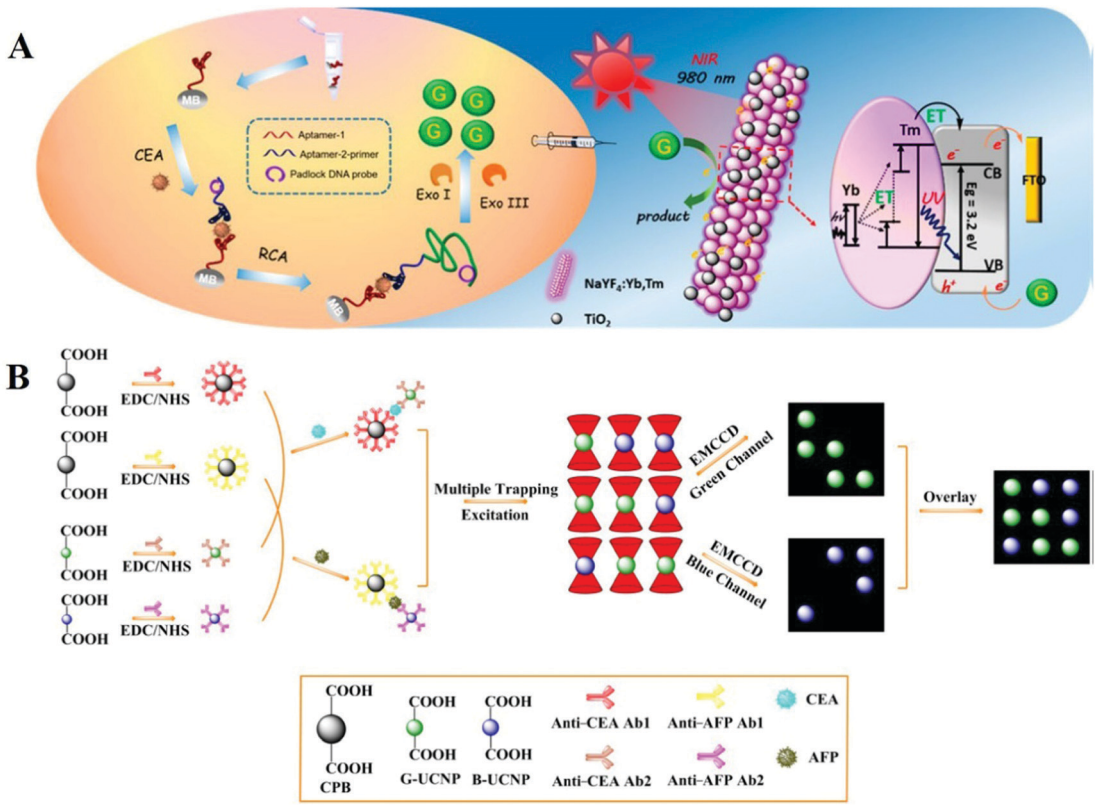

Fig. 3 (A) Schematic illustration of a sandwich platform for determination of target CEA based on UCNPs@TiO_2 microrods with rolling circle amplification upon irradiation with near-infrared light.[52] Copyright 2018, American Chemical Society. (B) Schematic showing the imaging-based suspension array by combining optical tweezers with upconversion luminescence for sensing CEA and alpha fetal protein with sandwich immunological recognition, where CEA and alpha fetal protein are monitored by green emission and blue emission signals, respectively.[53] Copyright 2018, American Chemical Society.

Carcinoembryonic antigen (CEA) is a kind of protein often linked with colorectal cancer. UCNPs combined with titanium dioxide upconversion microrods ($NaYF_4$:Yb,Tm@TiO_2) were designed for the detection of CEA[52] (Fig. 3A). The carcinoembryonic antigen was discovered on a magnetic bead by utilizing specific aptamers. Under optimal conditions, the UCNP-based aptamer sensing system can emit a distinct signal in response to CEA and enable the detection limit of CEA as 3.6 pg mL^{-1}. To meet the challenges of point-of-care detection and achieve the capability of multiplex detection, Tang's group reported an imageable suspension array based on UCNPs luminescence encoding for the determination of alpha fetal protein and CEA.[53] As shown in Fig. 3B, the different target binding processes are differentiated by using two species of UCNPs (B-UCNPs and G-UCNPs) as luminescent indicators, and a sandwich complex bead is made of carboxyl functionalized polystyrene beads. Using this bead assay, the detection limits of alpha fetal protein and CEA are 2.7 pg mL^{-1} and 3.1 pg mL^{-1}, respectively.

Prostate-specific antigen (PSA) as a biomarker of prostate cancer was detected by single-particle enumeration based on UCNPs and gold nanoparticles.[54] The carboxyl group-functionalized UCNPs decorated with anti-PSA detection antibodies play the role of energy donor, and gold nanoparticles conjugated with anti-PSA capture antibodies serve as the energy acceptor. In the presence of PSA, the immunoreaction drags UCNPs and gold nanoparticles into proximity, resulting in FRET between them, leading to luminescence quenching.

Jin's group designed UCNPs functionalized with a bispecific antibody to recognize the cancer antigen biomarker.[55] To achieve this, one end of the bispecific antibody was synthesized to recognize UCNPs, and the other end of the bispecific antibody was designed to conjugate the cancer antigen biomarker. By using the same strategy, Lan and co-workers synthesized UCNPs modified with a DNA aptamer sensor according to the structure of vascular endothelial growth factor (a biomarker of breast cancer).[56] In this system, the UCNPs were decorated with aptamer DNA by replacing the oleic acid on the surfaces. With the introduction of vascular endothelial growth factor, the upconversion luminescence signal was changed and detected upon irradiation with 980 nm light, leading to the determination of this biomarker with a detection limit of 6 pM. In these examples, UCNPs were decorated with functional moieties that can recognize biomolecules or play a role in energy transfer which results in luminescence change. Based on the luminescence change of UCNPs, the tumor biomarker 5-hydroxyindoleacetic acid was detected using a sensing probe comprised of silica spheres and UCNPs.[57] The sensing mechanism is based on the recovery of the fluorescence of UCNPs with the introduction of 5-hydroxyindoleacetic acid.

Apart from tumor biomarker detection, researchers also concentrate on designing luminescent sensors for cancer cell sensing. UCNPs combined with TiO_2/CdTe heterostructures were synthesized for use as a film electrode, and the aptamer AS1411 was linked to this electrode to specifically recognize breast cancer cells (MCF-7 cells).[58] In this system, the UCNPs convert near-infrared (NIR) light to visible light, which excites the semiconductor to improve the current response, resulting in the detection of MCF-7 cells ranging from 1×10^3 to 1×10^5 cells per mL. Guo *et al.* designed a luminescent lanthanide nanoprobe to detect circulating tumor cells,[59] which is a kind of blood biomarker for the evaluation of cancer metastasis and early cancer diagnosis. They first designed antibody-modified lanthanide nanoparticles ($NaEuF_4$–Ab) and microplate wells modified with anti-epithelial cell adhesion molecule antibodies. Owing to recognition between the antigens and antibodies of epithelial cell adhesion molecules, cancer cells can coordinate with $NaEuF_4$–Ab. Utilizing the time-resolved luminescence of these lanthanide particles, circulating tumor cells can be detected in the enhancer solution with a detection limit of 1 cell per well. Zhang's group also took advantage of time-resolved luminescence for sensing hepatocellular carcinoma.[60] They designed a tumor-microenvironment ($ONOO^-$)-responsive lanthanide–dye FRET sensor in which lanthanide nanoparticles serve as an energy donor, and the dye MY-1057 serves as an energy acceptor. The tumor areas can be differentiated from normal tissue according to the recovery lifetime.

2.3 Nucleic acids detection

Nucleic acids are large biological molecules usually located in cells, which are mainly responsible for the carrying and transmission of the genetic information of organisms. Nucleic acid analysis is very important in biological testing, genetics and molecular medicine. Researchers directly used upconversion luminescent materials as labeling reagents to detect single-stranded nucleic acids at early stages. For example, F van De Rijke *et al.* used UCNPs to detect nucleic acid hybrids on microarrays to obtain enhanced image contrast.[61] Corstjens *et al.* developed a system for detecting single-stranded DNA by covalently combining oligonucleotide probes with upconversion phosphors.[62] This low-sensitivity detection method limits the practical applications of nanosensors. So nanosensors based on the LRET effect have been developed. For example, Zhang's group designed a nucleotide sensor based on UCNPs.[63] In this system, the UCNPs act as energy donors, and another fluorophore acts as an energy acceptor. After the UCNPs are excited with NIR light, the energy is transferred to the fluorophore, which causes the fluorophore to emit light. Similarly, Li *et al.* chose gold nanoparticles (AuNPs) instead of organic fluorophores to act as energy acceptors for energy absorption, and used LRET between AuNPs and UCNPs to quench the fluorescence of UCNPs.[64] The nanosensor can detect miRNAs highly selectively in living cells through utilizing the circular dichroism and luminescence signal of the Au–UCNP pyramid. Zhu and co-workers designed a nanosystem in which lock-like DNA connects UCNPs and gold nanoparticles (AuNPs) together.[65] The upconversion emission is quenched through the LRET process. Multiple lock-like DNA can be repeatedly opened by a copy of a target microRNA with the help of the fuel hairpin DNA strand to trigger the separation of AuNPs from UCNPs. The detection limit of the nanoprobe is about 1000 times lower than that of the previously reported upconversion nanoprobe without signal amplification.

Nucleic acid sensing systems with high spatiotemporal resolution have been successfully constructed because of the

development of some highly sensitive sensors based on upconversion luminescence. This type of system can be used for both quantitative detection of nucleic acids and biological imaging *in vivo*. Li's group constructed an activatable DNA nanodevice that uses the high spatial and temporal precision of NIR light to detect miRNAs *in vivo*.[66] This nanodevice is functionalized on the surfaces of UCNPs through a DNA beacon, which can sense miRNA under UV light excitation. Later they focused their attention on the use of UCNPs to achieve signal amplification controlled by NIR light. They redesigned the functional unit of the hybridization chain reaction and combined it with UCNPs.[67] The hybridization chain reaction method excited by NIR light will enable signal amplification and imaging of RNA targets in living cells with high spatio-temporal accuracy.

2.4 Detection of other biomolecules

Other biomolecules such as neurotransmitters, antibiotics, and reactive oxygen species also play important roles in treating diseases and monitoring human physiological activity. Taking advantage of the multiple emission bands of UCNPs, Nezhad's group designed a multichannel sensor array for distinguishing four neurotransmitters: dopamine, levodopa, serotonin, and norepinephrine.[68] The fluorescent emission intensity of the UCNPs can be quenched by the oxidation products of the neurotransmitters with different levels under alkaline conditions. As a result, the multichannel emission intensity from the UCNPs selectively discriminates the neurotransmitters.

A ratiometric sensor which is designed with a ratio of two luminescent signals for self-calibration is a promising technique for measuring analytes especially in biological fluids, tissue samples, and live cells. Wang and co-workers designed a UCNP-based ratiometric probe (UCNP@RdMMSN@βCD) with two emission peaks at 540 and 656 nm for detecting nitric oxide in Oct-treated rat IR models[69] (Fig. 4A). The emission intensity ratio (I_{656}/I_{540}) of this system was investigated with the addition of NO and other reactive nitrogen and oxygen species (Fig. 4B). With the introduction of NO, the upconversion emission intensity at 656 nm remained stable, while the emission intensity at 540 nm decreased. In contrast, no obvious change was observed when this ratiometric probe was treated with other oxidative chemical species. Chen's group designed NIR dual-excitation ratiometric luminescence probes based on dye-sensitized UCNPs to detect hypochlorite in live MCF-7 cells[70] (Fig. 4C). The dye IR808, as a recognizer of hypochlorite in cells, is treated as an energy donor and UCNPs are used as an energy acceptor in this probe. With the introduction of NaClO, the luminescence intensity of IR808-UCNPs-F127 gradually decreased (Fig. 4D) upon 808 nm excitation. The upconversion luminescence signal excited using a 980 nm laser is not influenced by analytes, and thus can serve as a self-calibrated signal and alleviate the interference due to environmental

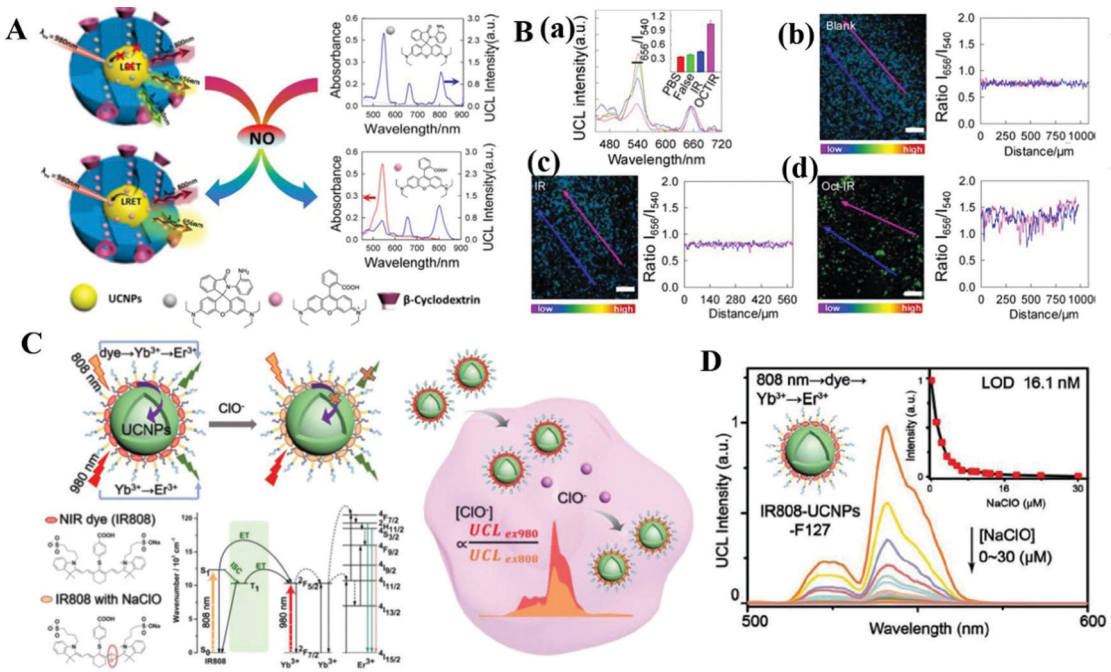

Fig. 4 (A) Schematic illustration of UCNPs for ratiometric sensing of nitric oxide.[69] Under 980 nm light excitation, the nanoprobe exhibits two luminescent emission signals at 540 nm and 656 nm. The UCNPs as the core are encapsulated within a shell of mesoporous SiO_2, where pores are filled with rhodamine B-derived molecules. (B) (a) Upconversion luminescence spectra and luminescence intensities (inset) of the probes. Error bars were from three parallel experiments. (b–d) Luminescence ratiometric photographs of rat liver tissue slices cultivated with the probes and the corresponding signal profile of a linear area across the rat liver slices under 980 nm excitation (the scale bar is 200 μm).[69] Copyright 2017, American Chemical Society. (C) Schematic showing the ratiometric sensing process of intracellular ClO^{-1} in a dye-sensitized UCNP probe and the corresponding analyte-dependent energy transfer mechanism.[70] (D) Upconversion luminescence spectra of the IR808-UCNPs-F127 probe with the introduction of NaClO under 808 nm excitation.[70] Copyright 2019, John Wiley & Sons.

change. The ratiometric probes improve detection accuracy *via* the self-calibration of two signal intensities, where one signal serves as a reference factor for adjusting another signal. Thus, the ratiometric detection is independent of sensor concentration and a variety of analyte-independent factors, leading to more reliable and accurate quantitation.

UCNPs integrated with other materials into one architecture for biomolecule sensing overcome some limitations of solo materials, which can improve the range of application and luminescence performance. Recently, Gu *et al.* reported an electrochemiluminescence sensor based on UCNP and covalent organic framework hybrid materials,[71] for monitoring dopamine in serum samples. The porous covalent organic framework-based electrochemiluminescent probe could load more UCNPs to enhance the luminescence intensity and imprint the recognition sites for dopamine determination. Recently, a sensor based on UCNPs encapsulated within metal organic frameworks (ZIF-8) and incorporating a molecularly imprinted polymer for discovering octopamine was synthesized by Fang's group.[25] The luminescence intensity and dispersity of UCNPs can be enhanced by the stability and high surface area of the MOFs under organic conditions, which can improve the detection limit for octopamine.

A solid-phase biosensor combined with Au nanocaps and UCNPs decorated with quencher-marked aptamers in a solid substrate was designed for the detection of ochratoxin A.[72] The upconversion luminescence of UCNPs can be quenched by the FRET between the quencher (aptamers) and UCNPs. Another example based on UCNP hybrid materials is that Au nanoparticles harvest light from UCNPs which convert NIR light into visible light, for sensing the concentration of reactive oxygen species.[73]

In recent work, a molecular imprinting technique is to attain the close interaction between the target molecule and UCNPs for rhodamine B sensing. The authors first synthesized UCNPs with a molecularly imprinted polymer at the surface where molecular cavities can selectively capture target molecules[74] with a detection limit of 6.27 μg mL^{-1}. Another example is that a fluorescent "double recognition" method combined with UCNPs and a molecular imprinting technique for detecting enrofloxacin to overcome conventional limitations of molecular imprinting including high cost, poor stability, and hard availability.[75] The UCNPs combined with the molecular imprinting technique can improve the interaction between biomolecules and UCNPs by shortening the distance between them, which is a useful method for specific targeting and detection of biomolecules.

The large superficial area of UCNPs may combine with numbers of biomolecules, resulting in a too dark or too light sensor in color. As a result, it is difficult to realize the color change with naked eyes. A placeholder strategy based on UCNPs was designed by Cheng and coauthors, to monitor dipicolinic acid (DPA), an acid anthrax biomarker.[76] The large surface area of UCNPs was partly occupied by sodium tripolyphosphate and eriochrome black T. In general, DPA displaces eriochrome black T from this nanosystem, which causes a color change from red to blue due to the release of free eriochrome black T into the solution. The detection limit of DPA is 0.9 μM, lower than the infectious dose of anthrax spores (60 μM).

3. Lanthanide downshifting luminescence for biomolecules detection

Lanthanide downshifting luminescence often means that the transformation from higher energy light to lower energy light.[77–80] Here, we mainly focus on the materials that emit visible light, like Ln-MOFs and lanthanide complexes. As the promising downshifting-luminescence materials, Ln-MOFs and lanthanide complexes have drawn intense attention in the sensing field for their high luminescence efficiency compared to UCNPs. In this part, we will introduce the recent developments of Ln-MOFs and lanthanide complexes for biomolecule detection.

3.1 Ln-MOF probes for biomolecules

Ln-MOFs as a subclass of MOFs not only exhibit the extraordinary luminescence properties of lanthanide ions but also exhibit the unique properties of MOFs,[76,81–84] such as high porosity, easy-modification and large surface area, which makes Ln-MOFs have great advantages in biosensing. Researchers can obtain various Ln-MOFs to detect different analytes by changing the organic ligands and replacing the lanthanide ions.

Antibiotics. Antibiotics are widely used in livestock farming and play important roles in human health due to their ability to kill or inhibit bacteria. The abuse of antibiotics in livestock contributes to bacterial drug resistance and antibiotic residues in meat products. Therefore, detecting antibiotics is quite essential for human health. A kind of Eu-MOF was obtained to selectively monitor sulfamethazine antibiotics.[59] The framework of Eu-MOF remained intact after the introduction of sulfamethazine, indicating that the quenching mechanism did not result from the structure collapse. Then the authors found that the possible mechanisms of Eu-MOF sensing for sulfamethazine are attributed to the inner-filter effect and dynamic quenching. To improve the detection limit and anti-interference performance of probes, Li and co-workers synthesized a ratiometric luminescence polynuclear Ln-MOF (Tb-L1) for detecting tetracycline antibiotics with a detection limit of 8 ng mL^{-1},[85] which are widely used for bacterial infection treatment in livestock as well as humans. In addition, this Tb-MOF can differentiate chlortetracycline, doxycycline, and oxytetracycline from tetracycline, because of the fingerprint relationship between tetracyclines and the emission peak-height ratio of lanthanide ions to the ligand.

To achieve rapid and cost-effective assays, Li *et al.* synthesized a $[Tb(HL)L(H_2O)]_n$ test stripe for sensing tetracycline antibiotics in aqueous solution.[86] Based on the quenching mechanism due to the inner filter effect, the tetracycline antibiotics can be sensitively detected using the $[Tb(HL)L(H_2O)]_n$ test stripe, and the detection limit for tetracycline antibiotics is 2.77 nM, comparable to that of the HPLC detection method. Based on photoinduced energy transfer between lanthanide ions and antibiotics, Wang *et al.* produced an Eu-MOF for the detection of metronidazole and dimetridazole antibiotics in aqueous solution and organic solution.[87] The detection limits of dimetridazole and metronidazole antibiotics are 13.4 ppm and 13.0 ppm, respectively, indicating that this Eu-MOF is promising in the diagnosis of antibiotic poisoning. Yu and

co-workers designed a ''turn-on'' luminescent probe based on an Eu-MOF,[88] for the detection of doxycycline, a polyketide antibiotic. The Eu-MOF was initially non-fluorescent; with the introduction of doxycycline, this probe showed obvious fluorescence improvement at 526 and 617 nm. Furthermore, the system can be successfully used as a sensing material for the detection of doxycycline in samples of urine and fish.

Dong *et al.* reported mixed membranes which are composed of $Eu_{1-x}Tb_x$-MOF and polymer materials,[89] further improving the flexibility of Ln-MOFs. In this study, Ln-MOFs were produced from europium/terbium nitrate and the ligand H_4L in DMA–H_2O solution at 100 °C. By changing the reactant time, submicrometer Ln-MOF (SMOF-10–10 h) spheres were obtained for easier and faster sensing applications. The luminescence experiments showed that the SMOF-10–10 h membrane had unique emission peaks of $Eu^{3+}$and Tb^{3+}ions that could detect different antibiotics in a certain concentration range on the basis of the emission ratio with I_{618}/I_{594} for Eu^{3+}ions (y-axis) and I_{544}/I_{489} for Tb^{3+}ions (x-axis) in a two dimensional map. With the increase of Tb^{3+}, the color of $Eu_{1-x}Tb_x$-MOF changed from magenta to green because Eu^{3+} ions were sensitized by Tb^{3+} ions.

Biomarkers. Detecting biomarkers of tumors and other diseases is of significance for early diagnosis and treatment. Some systems are based on the FRET mechanism, where the detection results depend on the fluorescence signal switch on/off. One example based on FRET to detect a cancer biomarker is Ln-MOF combined with silver nanoparticles which can sensitively detect miRNA-155[90] (Fig. 5A). When the energy is transferred to the noble metal, the energy will be consumed due to the plasmon resonance effect of Ag^+ ions, resulting in luminescence quenching. A water stable Eu-MOF was designed for detecting serotonin and 5-hydroxyindole-3-acetic acid,[91] which are biomarkers of carcinoid tumors. The quenching mechanism is attributed to the energy transfer effects as well as the dynamic quenching process. The FRET competition for the absorption of excitation laser radiation between the ligands and the analytes can hinder the energy transfer from the ligands to Eu^{3+} ions, resulting in luminescence quenching. The detection limits of serotonin and 5-hydroxyindole-3-acetic acid are 0.66×10^{-6} M and 0.54×10^{-6} M, respectively. Shi and coworkers reported R6H@Eu(BTC) as a colorimetric and ratiometric fluorescent probe for DPA with a detection limit of 4.5 μM,[92] a biomarker of Bacillus anthracis spores. The sensing mechanism was found as the emission signal quenching caused by FRET from Eu(BTC) to DPA and a transformation of the rhodamine structure caused by DPA.

Some examples are based on time-resolved techniques due to the long decay time of lanthanide ions, which can eliminate short-lived autofluorescence. Ln-MOF Eu–QPTCA was synthesized as a time-resolved luminescent probe for acute myocardial infarction which is an important cardiac biomarker; the detection limit of cardiac biomarker concentration was confirmed to be 1.0 U L^{-1}[93] (Fig. 5B). In this system, Eu^{3+} ions are sensitized by organic ligands and exhibit red emission under 373 nm light excitation. Interestingly, the red emission signal can be quenched by adenosine triphosphate (ATP), but less influenced by adenosine diphosphate (ADP). These different luminescent emission behaviors in response to ATP and ADP enable the Eu–QPTCA NMOFs to become luminescent probes for creatine kinase, a transformative switch between ATP and ADP.

In order to improve the sensing reliability of biomarkers, Li's group provided a facile technique to fabricate a semi-solid EuMOF-gel that can sense an endogenous metabolite called α-ketoglutaric acid in serum.[94] Almost at the same time, the same group provided another approach to tailor the performances of Eu–ZnMOF through structural engineering,[95] which can detect the concentration variation of urinary vanillylmandelic acid, an early pathological signature of pheochromocytoma.

Ascorbic acid. Ascorbic acid as a well-known antioxidant can react with many oxidants such as reactive oxygen species in the human body, and is important for the functions of organisms. Yue *et al.* designed a Ln-MOF that can detect ascorbic acid.[96] In this Ln-MOF, the luminescence intensity of Ce^{4+} ions (390 nm) increases and the emission peak (617 nm) of Eu^{3+} ions decreases with the increase of ascorbic acid concentration from 0 to 100 mM, resulting in a ratiometric luminescence sensor for ascorbic acid. The sensing mechanism is that ascorbic acid formed DHA after being oxidized by Ce^{4+}, which hinders the energy transfer from the organic framework to Eu^{3+} ions and results in the luminescence decrease of Eu^{3+} ions.

Amino acids. As we all know, amino acids play a significant role in all life activities. The detection of amino acids is essential

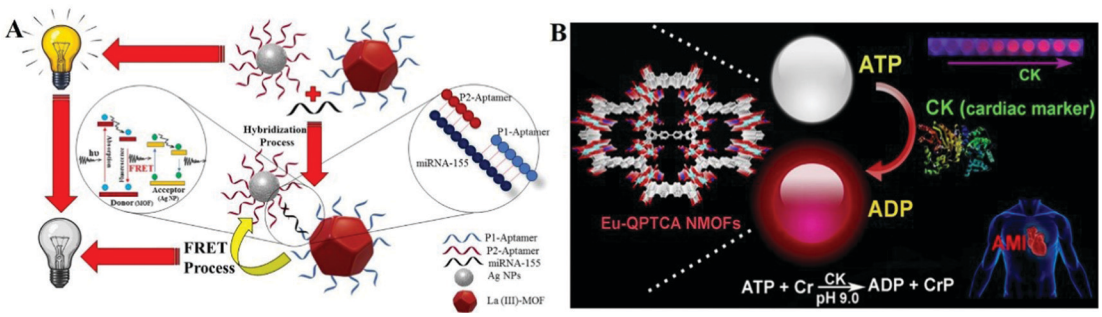

Fig. 5 (A) Schematic illustration of the luminescence quenching process of Ln(III)-MOF in response to miRNA-155 (a cancer biomarker) based on the FRET process.[90] Copyright 2020, American Chemical Society. (B) Schematic showing Eu–QPTCA NMOFs that acted as luminescent probes to detect creatine kinase (cardiac marker) activity.[93] Copyright 2019, American Chemical Society.

for body health, which can diagnose a variety of diseases in an early stage. Yan's group synthesized Ag^{+}@Eu-MOF to detect aspartic acid from a series of amino acids in aqueous solutions, and the detection limit is 0.46 μM.[97] In the presence of aspartic acid, the luminescence of Ag^{+}@Eu-MOF is associated with energy transfer between the ligand and Eu^{3+} and pH change, which causes a luminescence decrease of this hybrid material. Yang and co-workers reported an Eu-MOF that can distinguish aspartic acid and histidine from 14 amino acids with detection limits of 2.88 mM and 0.1 mM, repectively.[98] The sensing mechanism may result from energy transformation between the ligand and histidine and a dynamic process.

Due to the pH-related (pH 3–4) luminescence properties and the coordination effects from amino acids, Zhao and co-workers designed an Eu-MOF to monitor pH-related amino acids which can distinguish aspartic acid and glutamic acid from other amino acids with detection limits of 21 μM and 22.4 μM, respectively.[99] Corresponding to the above properties, the luminescence switching mechanism is due to the coordination of water molecules and the slight elongation of Eu–O bond, resulting in the luminescence quenching of the lanthanide ions. Using the same idea, Xiao and co-workers reported a pH-modulated system based on dually-emitting Eu^{3+}@Mn-MOF for detecting histidine.[100]

Other biomolecules. Gossypol, a natural toxin located in cottonseeds, threatens the safety of cottonseed products. Owing to the complexity of the sensing environment, it is difficult to detect gossypol with a "turn-off" pattern. Luo *et al.* designed a Yb-NH_2-TPDC system that produces a unique emission peak of Yb^{3+} ions under 485 nm excitation with the addition of gossypol,[101] resulting in sensing the gossypol concentration of 0.5–100 μg mL^{-1} in acetone solution (Fig. 6A). The luminescence process is attributed to the antenna effect of gossypol for Yb^{3+} ions, which transfers energy from the ligand to metal ions. With the addition of gossypol, the luminescence intensity of Yb-NH_2-TPDC at 976 nm increased upon 485 nm excitation (Fig. 6B and C). The sensing system based on a MOF generally consumes long periods because analytes enter into the pores of the MOF *via* the permeation process. In order to rapidly detect gossypol, they also explored $YbCl_3{\cdot}6H_2O$ solution and got a similar result. The sensing pattern of most biosensors was based on a "turn-off" switch, yet "turn-on" switch sensors have lots of advantages for many analytes. For example, "turn-off" probes can be easily influenced by the surrounding environment such as pH, solvents and temperature, resulting in the inaccuracy of the luminescence signal. However, analytes coordinate and sensitize the lanthanide ions as ligands to fabricate an effective "turn-on" switch, which can prompt the sensing system from the dark to light emission state or adjust the luminescence color. Another case based on a "turn-on" switch was reported by Wang and co-workers;[102] an Eu-MOF that can monitor the concentration of levofloxacin in serum and urine within one minute was synthesized. However, the mechanism of the "turn-on" luminescent switch was not given.

3.2 Lanthanide complex probes for biomolecules

Luminescent lanthanide complexes have gained increasing attention in bioanalytical studies,[103–106] especially those of europium ions and terbium ions. Lanthanide complexes have several advantages over conventional fluorophores in sensing applications, such as a large distance between emission and absorption spectra, which can reduce excitation light interference, the long luminescence lifetimes which allow time-gated detection techniques and the emission spectra with defined bands that permit ratiometric analyses.

Several principles for designing efficient luminescent lanthanide complexes need to be considered. Firstly, it is difficult to directly excite lanthanide ions because of their Laporte forbidden property of the f–f transitions. However, the lanthanide complexes with efficient luminescence can be achieved by coordinating the lanthanide ions with a strongly absorbing antenna ligand. Secondly, lanthanide ions need to accept sufficient energy from the antenna ligand, so the energy gap between the triplet state of the ligand and the accepting energy levels of the lanthanide ions should be appropriate. Thirdly, lanthanide ions adopt coordination numbers between 7 and 10; as a result, the antenna ligand should have a sufficient number of donors to surround the lanthanide sphere.

Instead of classifying the analytes by species, we will define lanthanide complex probes by the categories of sensing strategies, such as the time-gated technique and ratiometric analyses, which can meet requirements in face of practical challenges.

Time-gated technique. The time-gated technique based on the long decay time of lanthanide ions was used for rapid

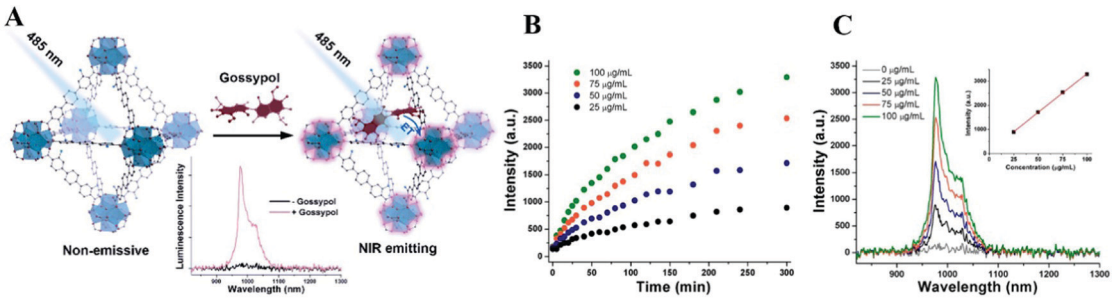

Fig. 6 (A) Schematic illustration of the luminescence "turn-on" process of Yb-NH_2-TPDC for the detection of gossypol under 485 nm excitation. (B) Kinetics of the luminescence intensity of Yb-NH_2-TPDC at 976 nm at different gossypol concentrations (λ_{ex} = 485 nm). (C) Emission spectra of Yb-NH_2-TPDC in gossypol solutions at different concentrations at 300 min. The inset diagram shows the calibration curve (λ_{ex} = 485 nm).[101] Copyright 2020, American Chemical Society.

detection of reactive oxide species such as hypochlorous acid.[107] The lanthanide complex [Eu(L)$_3$(DPBT)] was synthesized, which showed low cytotoxicity in living cells. The long luminescence lifetime of [Eu(L)$_3$(DPBT)] allows it to be applied for the time-gated luminescence response and imaging of hypochlorous acid formation in inflammatory cells. In order to extend its use to practical application, the authors immobilised the sensor in a PEG hydrogel, which can rapidly detect hypochlorous acid generation and differentiate acute wounds from slight ones. Another example based on time-gated technology is that Guo *et al.* reported a simple probe that utilized the FRET between terbium ions and Cy5.5 for microRNA detection.[108] They achieved multiplexed detection results of different targets from the same microRNA sample by using different luminescence windows of Tb-Cy5.5 at a single excitation wavelength. Brennecke and co-workers also designed a Tb complex as a turn-on luminescent sensor for time-gated sensing of nitroreductases.[109] The nitroreductases as antenna ligands are able to combine the Tb^{3+} center and transfer energy to Tb^{3+} ions, which turns this non-fluorescent system into the one featuring fluorescent signals upon activation. Using the unique properties of lanthanide ions properly can offer great enhancement for analyte detection in different circumstances.

There are many strategies to break the limitation of the lanthanide complex and have better effects in biomolecule detection. For example, to improve the detection limit of carcinoembryonic antigen (an important tumor marker in prognosis and clinical diagnosis), Chen's group replaced the Eu complex by using Eu micelles (Eu_2O_3@PAA) which can produce thousands of Eu^{3+} ions (Fig. 7A).[110] This strategy takes advantage of dissolution-enhanced luminescence amplification. After the introduction of enhancer solution, the luminescence intensity (Fig. 7B) and lifetime (Fig. 7C) of PAA-capped Eu_2O_3 increased. The luminescent signal was measured by time-resolved technology to quantitatively monitor the concentration of carcinoembryonic antigen in saliva with a detection limit of 1.47 pg mL^{-1}. Furthermore, upon illumination with UV light (365 nm), the luminescent signal of Eu_2O_3@PAA can be seen clearly in enhancer solution with naked eyes, but a weak signal in PBS solution (Fig. 7B, inset).

Ratiometric luminescence analyses. The line-like emission spectra of lanthanide complexes permit ratiometric analyses, which offer self-calibration of signal correction, leading to reliable detection results. DPA, a major and unique component of anthrax spores (an anthrax biomarker), is harmful to humans and animals and can coordinate Tb^{3+} and Eu^{3+} to form a hybrid complex. Zhang's group developed dual lanthanide complexes (Tb/DPA@SiO_2−Eu/GMP) as a ratiometric fluorescent sensor for monitoring the DPA biomarker.[111] A Tb complex (Tb/DPA@SiO_2) was first synthesized and modified with amino (Fig. 8A), which can emit green luminescence with the addition of DPA performing the antenna effect (at an excitation wavelength of

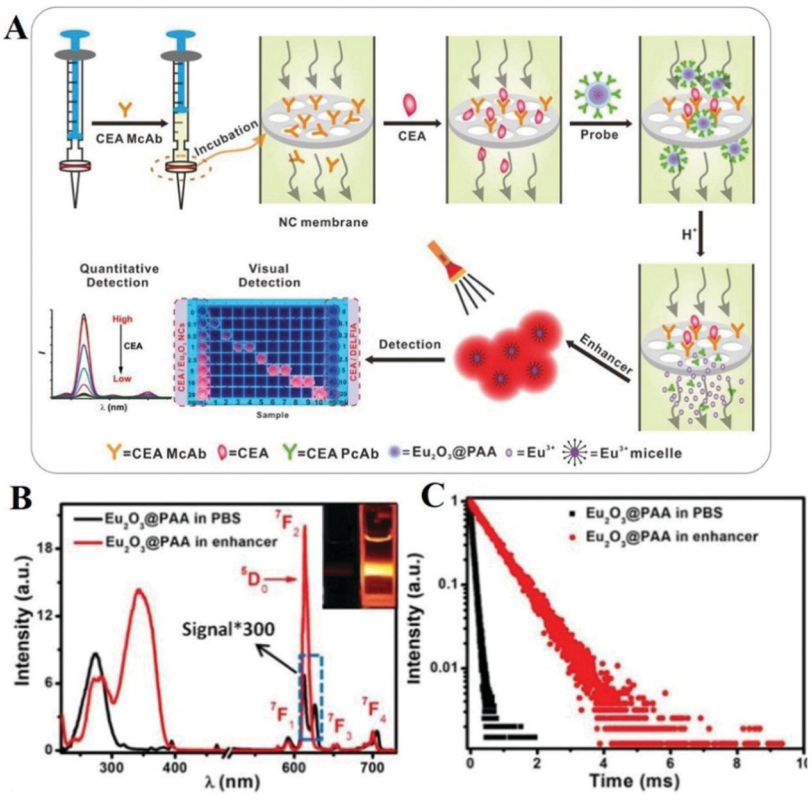

Fig. 7 (A) Schematic showing CEA detection *via* Eu_2O_3@PAA in saliva. Eu_2O_3 nanocrystals and a syringe filter are used as nanoprobes and a bioassay platform, respectively. The bioassay allows time-resolved and visual sensing of CEA. (B) Excitation spectra (left) and emission spectra (right) of Eu_2O_3@PAA in PBS solution and enhancer solution, respectively. Insets show the luminescent photographs of Eu_2O_3@PAA in PBS solution (left) and enhancer solution (right) with 365 nm light excitation. (C) Luminescence lifetime decays of Eu_2O_3@PAA in PBS solution and enhancer solution, respectively.[110] Copyright 2021, John Wiley & Sons.

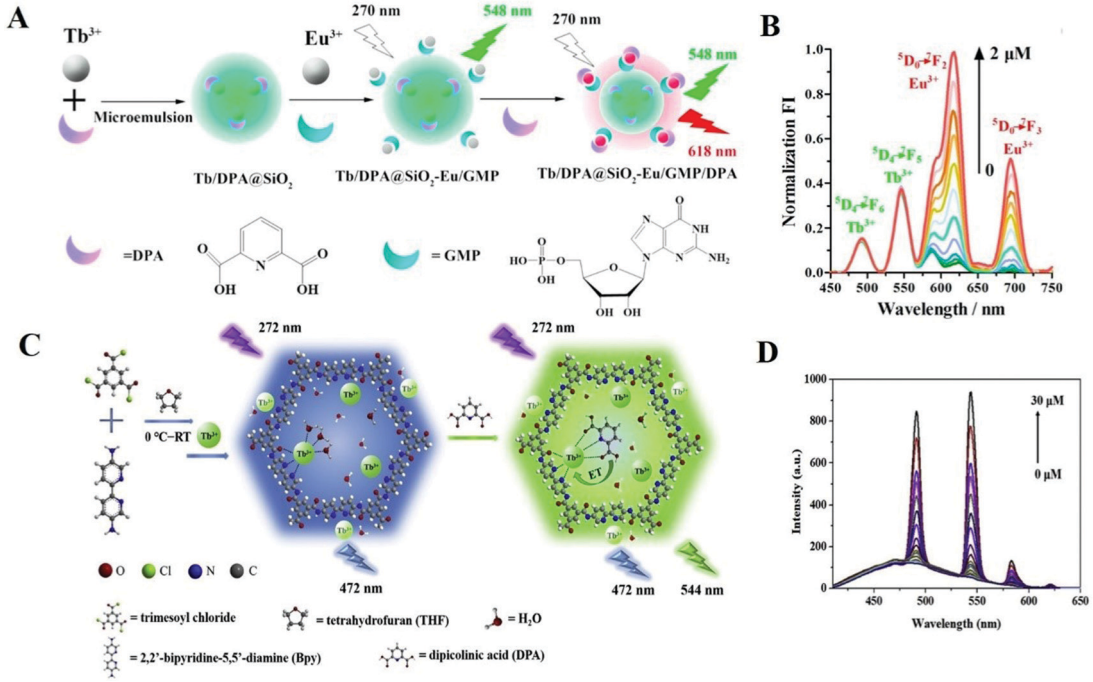

Fig. 8 (A) Schematic representation of ratiometric Tb/DPA@SiO_2–Eu/GMP complexes for DPA detection.[111] Copyright 2017, Elsevier. (B) Fluorescent emissions of the Tb/DPA@SiO_2–Eu/GMP probe with increase in DPA concentration (0–2.0 μM) (λ_{ex} = 272 nm). (C) Schematic illustration of a ratiometric fluorescent Tb-COP complex and the process for DPA detection.[112] Copyright 2019, Elsevier. (D) Fluorescence intensities of Tb-COP with different concentrations of DPA (0–30 μM) under 272 nm excitation.

270 nm). Then, Tb/DPA@SiO_2 was embedded into the network matrix of Eu/GMP coordination polymers to fabricate Tb/DPA@SiO_2–Eu/GMP lanthanide complexes. In the presence of DPA, Tb/DPA@SiO_2–Eu/GMP/DPA assembled and excluded water from Eu^{3+} ions, which can enhance the red signal of this system (Fig. 8B). Using the long decay time of lanthanide ions, this system can serve as a time-resolved ratiometric fluorescent sensor for DPA with a detection limit of approximately 1 μM. Jia's group reported a terbium-covalent organic polymer (Tb-COP) (Fig. 8C),[112] a ratiometric fluorescent sensor for DPA with a detection limit of 13.5 nM, which is much lower than that of the former example. In this system, COP was synthesized by an amidation reaction of 2,2′-bipyridine-5,5′-diamine with trimesoyl chloride, and Tb^{3+} was conjugated with COP to form a ratiometric probe for sensing DPA. With the addition of DPA at different concentrations, the luminescent signal of Tb-COP changed (Fig. 8D) upon 272 nm illumination. In this system, the luminescent signal of COP was applied as a luminescent contrast for Tb^{3+}, which acted as a response signal. The sensing process of this Tb-COP is that DPA plays the role of antenna and transfers energy to Tb^{3+}.

In addition to Tb^{3+}, Eu^{3+} ions can also coordinate with DPA and form Eu complexes. Donmez *et al.* synthesized a ratiometric probe based on an EDTA–Eu^{3+} complex and fluorescein dye,[113] for detecting DPA as well (detection limit = 10 nM). This probe takes advantage of the coordination ability of DPA with Eu^{3+}, forming a luminescent EDTA–Eu^{3+}/DPA complex. In this ratiometric fluorescent probe, the EDTA–Eu^{3+} is the sensing part, and fluorescein dye is the internal reference. The luminescent intensity of fluorescein dye remained constant when the Eu^{3+} emission increased with the addition of DPA. Using the same idea, Tang's group designed a nanoprobe based on a terbium functionalized micelle and a fluorophore for DPA detection; the detection limit is 54 nM.[114] The Tb^{3+} ions in the micelle can be sensitized to emit unique luminescence with the introduction of DPA. The luminescence intensity of the fluorophore remained constant, resulting in ratiometric luminescence response for DPA. Recently, the same group reported Eu^{3+}/Tb^{3+} hybrids for ratiometric detection of DPA (detection limit = 27.3 nM). Instead of using a fluorophore as fluorescence reference, they took advantage of the intrinsic emission peaks of Tb^{3+} (545 nm) and Eu^{3+} (613 nm) as the luminescence ratio (excitation wavelength: 280 nm).[115] Both the fluorescence lifetimes and intensities of the luminescence ratio I_{545}/I_{613} maintain a good correlation upon addition of DPA, which prove that these Eu^{3+}/Tb^{3+}hybrids as probes have a good sensing ability towards DPA.

As we can see from the examples mentioned above, use of analytes as ligands to coordinate lanthanide centers is an important strategy to fabricate luminescent sensors where lanthanide ions absorb energy from analytes and emit the characteristic fluorescence signal of lanthanide ions. Luminescent labels combined with other fluorophores can serve as ratiometric probes to achieve reliable and sensitive results.

4. Summary and outlook

In conclusion, we summarized recent advancements of Ln^{3+}-containing luminescent probes in sensitive and selective

sensing biomolecules. These research studies reveal that Ln^{3+}-containing luminescent probes have drawn extensive attention in recent years due to their outstanding physicochemical characteristics, enabling them to become intriguing candidates for biosensing. To explore the full potential of Ln^{3+}-containing luminescent probes, researchers are making their efforts to expand the category of detectable targets, discover novel methodologies, and improve the selectivity and sensitivity of the probes towards biomolecules. Although some substantial advances of the probes have been made due to their ingenious design strategies, several challenges still remain to meet the requirements toward commercial applications.

First, although the sensitivity and selectivity of current luminescent probes are usually adequate for sensing single analytes, more efforts should be made towards the development of diversified systems which can monitor multiple biomolecules at the same time. Lifetime-based lanthanide luminescent probes are receiving increasing attention in multiplexed biosensing, which can eliminate signal distortion under biological conditions. Nevertheless, strategies for lifetime-based probes with sensitivity, selectivity, and fast feedback are lacking in exploiting. To achieve multiplexed sensing, more attention should be paid to working on the controlled lifetime responsiveness and precise synthesis of probes.

Second, the low upconversion luminescence efficiencies of UCNPs have been a key bottleneck for a long time, which may cause low sensitivity of biosensing and poor resolution. As a result, novel strategies to fabricate UCNPs for biosensing with high quantum efficiency are much needed. The UCNPs combined with other materials have become one of the promising methods for sensing, which can tackle some drawbacks of solo optical labels and fully take advantage of the merits of UCNPs and traditional fluorophores to obtain high quantum efficiencies of lanthanide nanoparticles. For example, the system of UCNPs conjugated with organic molecules can take advantage of the high light-absorption ability of organic molecules and then transfer energy to UCNPs, enhancing the luminescence efficiencies of the whole system.

Third, as of now, the long-term toxicity of UCNPs is another bottleneck for *in vivo* sensing of biomolecules, though a variety of surface modification approaches have been employed to alter the stability and toxicity of UCNPs. It is necessary to discover novel lanthanide upconversion materials. Recently, molecular upconversion was investigated, in which photons with high energy are emitted upon excitation of molecular or supramolecular systems with photons with low energy.[116,117] These upconversion systems at the molecular level are a promising direction to overcome the constraint of UCNPs.

Fourth, for lanthanide complexes and Ln-MOFs, challenges including their short excitation wavelengths and low water solubility still exist for the detection of biomolecules. Here we propose some potential strategies in the design and development of multifunctional lanthanide probes for biomolecules: (i) developing new design rationales; (ii) exploiting probes based on ratiometric luminescence and time-resolved techniques – both the ratiometric assays and time-resolved techniques can greatly eliminate the influences due to environmental factors, resulting in reliable and sensitive detection; and (iii) combining other fluorophores with lanthanide complexes or Ln-MOFs, which can significantly improve the luminescent properties and functionality to meet the requirements of commercial applications.

Luminescent lanthanide-based systems including UCNPs, lanthanide complexes, and Ln-MOFs for biomolecule detection not only inspire researchers to study the advantages of different fluorophores but also enlighten researchers to discover new directions between luminescence science and biosensing. In addition, to meet different challenges in commercial applications, developing hybrid materials which can take full advantage of the potential properties of each material should be considered. We hope this review will broaden the horizons of the wider scientific groups about how to design and synthesize all kinds of hybrid systems for biomolecule detection.

Author contributions

G. S., H. Z. and L. S. drafted the article framework. G. S., Y. X., and L. S. searched and read the references, and wrote and revised the paper. H. Z. and L. S. supervised the process. All authors proofread, commented on, and approved the final submitted version of the manuscript.

Conflicts of interest

The authors declare no competing interest.

Acknowledgements

We are grateful for the financial support from the National Natural Science Foundation of China (Grant No. 51872183), the ''Shuguang Scholar'' of Shanghai Municipal Education Commission (19SG38), and the project from the State Key Laboratory of Rare Earth Resources Utilization (RERU2016013).

Notes and references

1 J. Zhou, Q. Liu, W. Feng, Y. Sun and F. Li, *Chem. Rev.*, 2015, **115**, 395–465.
2 L. Sun, R. Wei, J. Feng and H. Zhang, *Coord. Chem. Rev.*, 2018, **364**, 10–32.
3 X. Zhu, J. Zhang, J. Liu and Y. Zhang, *Adv. Sci.*, 2019, **6**, 1901358.
4 Y. Fan and F. Zhang, *Adv. Opt. Mater.*, 2019, **7**, 1801417.
5 B. Zhou, L. Yan, J. Huang, X. Liu, L. Tao and Q. Zhang, *Nat. Photonics*, 2020, **14**, 760–766.
6 X. Ou, X. Qin, B. Huang, J. Zan, Q. Wu, Z. Hong, L. Xie, H. Bian, Z. Yi, X. Chen, Y. Wu, X. Song, J. Li, Q. Chen, H. Yang and X. Liu, *Nature*, 2021, **590**, 410–415.
7 Z. Zhang, S. Shikha, J. Liu, J. Zhang, Q. Mei and Y. Zhang, *Anal. Chem.*, 2019, **91**, 548–568.

8 K. Staszak, K. Wieszczycka, V. Marturano and B. Tylkowski, *Coord. Chem. Rev.*, 2019, **397**, 76–90.
9 Y. Weng, Q. Zhu, Z. Z. Huang and H. Tan, *ACS Appl. Mater. Interfaces*, 2020, **12**, 30882–30889.
10 S. E. Bodman and S. J. Butler, *Chem. Sci.*, 2021, **12**, 2716–2734.
11 T. K. Mondal, S. Mondal, U. K. Ghorai and S. K. Saha, *J. Colloid Interface Sci.*, 2019, **553**, 177–185.
12 G. Sun, J. Tang, C. D. Snow, Z. Li, Y. Zhang, Y. Wang and L. A. Belfiore, *Cryst. Growth Des.*, 2019, **19**, 5658–5664.
13 Y. Liu, G. Bai, Y. Lyu, Y. Hua, R. Ye, J. Zhang, L. Chen, S. Xu and J. Hao, *ACS Nano*, 2020, **14**, 16003–16012.
14 X. Yang, H. Zou, X. Sun, T. Sun, C. Guo, Y. Fu, C. M. L. Wu, X. Qiao and F. Wang, *Adv. Opt. Mater.*, 2019, **7**, 1900336.
15 W. Yan, C. Zhang, S. Chen, L. Han and H. Zheng, *ACS Appl. Mater. Interfaces*, 2017, **9**, 1629–1634.
16 M. I. Halawa, B. S. Li and G. Xu, *ACS Appl. Mater. Interfaces*, 2020, **12**, 32888–32897.
17 J. Wang, J. Liu, J. Wang, Y. Wang, J. Cao, L. Hou, R. Ge, J. Chi, L. Huang, J. Guo, A. R. Aleem, Z. Song, S. K. Tamang, J. Liu, G. Wang, M. J. Kipper, L. A. Belfiore and J. Tang, *J. Mater. Chem. C*, 2020, **8**, 8171–8182.
18 J. Mu, L. He, P. Huang and X. Chen, *Coordin. Chem. Rev.*, 2019, **399**, 213039.
19 Y. Manmana, T. Kubo and K. Otsuka, *TrAC, Trends Anal. Chem.*, 2021, **135**, 116160.
20 X. Qian and B. Städler, *Adv. Funct. Mater.*, 2020, **30**, 2004605.
21 A. John-Herpin, D. Kavungal, L. von Mucke and H. Altug, *Adv. Mater.*, 2021, **33**, 2006054.
22 H. Liu and Y. Lei, *Biosens. Bioelectron.*, 2021, **177**, 112901.
23 R. Geng, R. Chang, Q. Zou, G. Shen, T. Jiao and X. Yan, *Small*, 2021, **17**, 2008114.
24 X.-L. Yang, R.-B. Zang, R. Shao, R.-F. Guan and M.-H. Xie, *J. Hazard. Mater.*, 2021, **413**, 125467.
25 Y. Cao, X. Hu, T. Zhao, Y. Mao, G. Fang and S. Wang, *Sens. Actuators, B*, 2021, **326**, 128838.
26 Y. Zhao, Q. Wang, H. Wang, H. Zhangsun, X. Sun, T. Bu, Y. Liu, W. Wang, Z. Xu and L. Wang, *Sens. Actuators, B*, 2021, **334**, 129610.
27 T. Singha Mahapatra, A. Dey, H. Singh, S. S. Hossain, A. K. Mandal and A. Das, *Chem. Sci.*, 2020, **11**, 1032–1042.
28 X. Ge, R. Wei and L. Sun, *J. Mater. Chem. B*, 2020, **8**, 10257–10270.
29 M. Zhao, B. Li, H. Zhang and F. Zhang, *Chem. Sci.*, 2021, **12**, 3448–3459.
30 K. Wieszczycka, K. Staszak, M. J. Woźniak-Budych and S. Jurga, *Coord. Chem. Rev.*, 2019, **388**, 248–267.
31 G. Chen, H. Qiu, P. N. Prasad and X. Chen, *Chem. Rev.*, 2014, **114**, 5161–5214.
32 R. Deng, J. Wang, R. Chen, W. Huang and X. Liu, *J. Am. Chem. Soc.*, 2016, **138**, 15972–15979.
33 Y. Zhang, S. Xu, X. Li, J. Zhang, J. Sun, L. Tong, H. Zhong, H. Xia, R. Hua and B. Chen, *Sens. Actuators, B*, 2018, **257**, 829–838.
34 J. Zhou, C. Li, D. Li, X. Liu, Z. Mu, W. Gao, J. Qiu and R. Deng, *Nat. Commun.*, 2020, **11**, 4297.
35 Z. Li, H. Liu, H. Li, Y.-H. Tsou, Y. Gao, X. Xu, W. Du, L. Wei and M. Yu, *Sens. Actuators, B*, 2019, **280**, 94–101.
36 J. Su, Y. Li, W. Gu and X. Liu, *RSC Adv.*, 2020, **10**, 26664–26670.
37 J. Zheng, Y. Wu, D. Xing and T. Zhang, *Nano Res.*, 2019, **12**, 931–938.
38 T. Liang, Z. Li, P. Wang, F. Zhao, J. Liu and Z. Liu, *J. Am. Chem. Soc.*, 2018, **140**, 14696–14703.
39 T. Guo, Q. Deng, G. Fang, Y. Yun, Y. Hu and S. Wang, *Biosens. Bioelectron.*, 2016, **85**, 596–602.
40 L. Liu, H. Zhang, Z. Wang and D. Song, *Biosens. Bioelectron.*, 2019, **141**, 111403.
41 Y. You, S. Cheng, L. Zhang, Y. Zhu, C. Zhang and Y. Xian, *Anal. Chem.*, 2020, **92**, 5091–5099.
42 M. Gao, R. Wu, Q. Mei, C. Zhang, X. Ling, S. Deng, H. He and Y. Zhang, *ACS Sens.*, 2019, **4**, 2864–2868.
43 M. Negahdary, *Biosens. Bioelectron.*, 2020, **152**, 112018.
44 L. Wu and X. Qu, *Chem. Soc. Rev.*, 2015, **44**, 2963–2997.
45 R. L. Siegel, K. D. Miller and A. Jemal, *Ca-Cancer J. Clin.*, 2016, **66**, 7–30.
46 R. Ben-Hamo, A. Jacob Berger, N. Gavert, M. Miller, G. Pines, R. Oren, E. Pikarsky, C. H. Benes, T. Neuman, Y. Zwang, S. Efroni, G. Getz and R. Straussman, *Nat. Commun.*, 2020, **11**, 3296.
47 J. Li, C. Ji, B. Lu, M. Rodin, J. Paradies, M. Yin and D. Kuckling, *ACS Appl. Mater. Interfaces*, 2020, **12**, 36873–36881.
48 Y. Wang, S. Zeng, A. Crunteanu, Z. Xie, G. Humbert, L. Ma, Y. Wei, A. Brunel, B. Bessette, J.-C. Orlianges, F. Lalloué, O. G. Schmidt, N. Yu and H.-P. Ho, *Nano-Micro Lett.*, 2021, **13**, 96.
49 G. Yang, Z. Xiao, C. Tang, Y. Deng, H. Huang and Z. He, *Biosens. Bioelectron.*, 2019, **141**, 111416.
50 S. Yadav, N. Kashaninejad, M. K. Masud, Y. Yamauchi, N. T. Nguyen and M. J. A. Shiddiky, *Biosens. Bioelectron.*, 2019, **139**, 111315.
51 G. S. Perera, T. Ahmed, L. Heiss, S. Walia, M. Bhaskaran and S. Sriram, *Small*, 2021, **17**, 2005582.
52 Z. Qiu, J. Shu and D. Tang, *Anal. Chem.*, 2018, **90**, 1021–1028.
53 C. Y. Li, D. Cao, C. B. Qi, Y. F. Kang, C. Y. Song, D. D. Xu, B. Zheng, D. W. Pang and H. W. Tang, *Anal. Chem.*, 2018, **90**, 2639–2647.
54 X. Li, L. Wei, L. Pan, Z. Yi, X. Wang, Z. Ye, L. Xiao, H. W. Li and J. Wang, *Anal. Chem.*, 2018, **90**, 4807–4814.
55 H. He, C. B. Howard, Y. Chen, S. Wen, G. Lin, J. Zhou, K. J. Thurecht and D. Jin, *Anal. Chem.*, 2018, **90**, 3024–3029.
56 J. Lan, L. Li, Y. Liu, L. Yan, C. Li, J. Chen and X. Chen, *Microchim. Acta*, 2016, **183**, 3201–3208.
57 D. Wang and E. Sun, *Microporous Mesoporous Mater.*, 2020, **299**, 110131.
58 K. Wang, R. Zhang, N. Sun, X. Li, J. Wang, Y. Cao and R. Pei, *ACS Appl. Mater. Interfaces*, 2016, **8**, 25834–25839.
59 K. Ren, S. H. Wu, X. F. Guo and H. Wang, *Inorg. Chem.*, 2019, **58**, 4223–4229.
60 M. Zhao, B. Li, Y. Wu, H. He, X. Zhu, H. Zhang, C. Dou, L. Feng, Y. Fan and F. Zhang, *Adv. Mater.*, 2020, **32**, 2001172.

61 A. Olesund, V. Gray, J. Martensson and B. Albinsson, *J. Am. Chem. Soc.*, 2021, **143**, 5745–5754.
62 P. Bharmoria, H. Bildirir and K. Moth-Poulsen, *Chem. Soc. Rev.*, 2020, **49**, 6529–6554.
63 Z. Li, Y. Zhang and S. Jiang, *Adv. Mater.*, 2008, **20**, 4765–4769.
64 S. Li, L. Xu, W. Ma, X. Wu, M. Sun, H. Kuang, L. Wang, N. A. Kotov and C. Xu, *J. Am. Chem. Soc.*, 2016, **138**, 306–312.
65 K. Zhang, L. Yang, F. Lu, X. Wu and J. J. Zhu, *Small*, 2018, **14**, 1703858.
66 J. Zhao, H. Chu, Y. Zhao, Y. Lu and L. Li, *J. Am. Chem. Soc.*, 2019, **141**, 7056–7062.
67 H. Chu, J. Zhao, Y. Mi, Y. Zhao and L. Li, *Angew. Chem., Int. Ed.*, 2019, **58**, 14877–14881.
68 S. Abbasi-Moayed, A. Bigdeli and M. R. Hormozi-Nezhad, *ACS Appl. Mater. Interfaces*, 2020, **12**, 52976–52982.
69 N. Wang, X. Yu, K. Zhang, C. A. Mirkin and J. Li, *J. Am. Chem. Soc.*, 2017, **139**, 12354–12357.
70 J. Ke, S. Lu, X. Shang, Y. Liu, H. Guo, W. You, X. Li, J. Xu, R. Li, Z. Chen and X. Chen, *Adv. Sci.*, 2019, **6**, 1901874.
71 Y. Gu, J. Wang, H. Shi, M. Pan, B. Liu, G. Fang and S. Wang, *Biosens. Bioelectron.*, 2019, **128**, 129–136.
72 K. Kim, E. J. Jo, K. J. Lee, J. Park, G. Y. Jung, Y. B. Shin, L. P. Lee and M. G. Kim, *Biosens. Bioelectron.*, 2020, **150**, 111885.
73 W. L. Wan, B. Tian, Y. J. Lin, C. Korupalli, M. Y. Lu, Q. Cui, D. Wan, Y. Chang and H. W. Sung, *Nat. Commun.*, 2020, **11**, 534.
74 L. Yang, X. Chen, P. Ma, D. Jin, J. Zhou, H. He, Z. Cheng and J. Lin, *Dalton Trans.*, 2020, **49**, 17200–17206.
75 X. Liu, J. Ren, L. Su, X. Gao, Y. Tang, T. Ma, L. Zhu and J. Li, *Biosens. Bioelectron.*, 2017, **87**, 203–208.
76 Z. H. Cheng, X. Liu, S. Q. Zhang, T. Yang, M. L. Chen and J. H. Wang, *Anal. Chem.*, 2019, **91**, 12094–12099.
77 A. S. Hyre and L. H. Doerrer, *Coord. Chem. Rev.*, 2020, **404**, 213098.
78 J. Feng and H. Zhang, *Chem. Soc. Rev.*, 2013, **42**, 387–410.
79 P. Reineck and B. C. Gibson, *Adv. Opt. Mater.*, 2017, **5**, 1600446.
80 M. Tan, F. Li, N. Cao, H. Li, X. Wang, C. Zhang, D. Jaque and G. Chen, *Small*, 2020, **16**, 2004118.
81 P. F. Muldoon, G. Collet, S. V. Eliseeva, T. Y. Luo, S. Petoud and N. L. Rosi, *J. Am. Chem. Soc.*, 2020, **142**, 8776–8781.
82 Z. W. Jiang, Y. C. Zou, T. T. Zhao, S. J. Zhen, Y. F. Li and C. Z. Huang, *Angew. Chem., Int. Ed.*, 2020, **59**, 3300–3306.
83 S. L. Anderson, D. Tiana, C. P. Ireland, G. Capano, M. Fumanal, A. Gładysiak, S. Kampouri, A. Rahmanudin, N. Guijarro, K. Sivula, K. C. Stylianou and B. Smit, *Chem. Sci.*, 2020, **11**, 4164–4170.
84 M. Zeng, A. Ren, W. Wu, Y. Zhao, C. Zhan and J. Yao, *Chem. Sci.*, 2020, **11**, 9154–9161.
85 R. Li, W. Wang, E.-S. M. El-Sayed, K. Su, P. He and D. Yuan, *Sens. Actuators, B*, 2021, **330**, 129314.
86 C. Li, C. Zeng, Z. Chen, Y. Jiang, H. Yao, Y. Yang and W. T. Wong, *J. Hazard. Mater.*, 2020, **384**, 121498.
87 G.-D. Wang, Y.-Z. Li, W.-J. Shi, B. Zhang, L. Hou and Y.-Y. Wang, *Sens. Actuators, B*, 2021, **331**, 129377.
88 L. Yu, H. Chen, J. Yue, X. Chen, M. Sun, J. Hou, K. A. Alamry, H. M. Marwani, X. Wang and S. Wang, *Talanta*, 2020, **207**, 120297.
89 J. Dong, S. L. Hou and B. Zhao, *ACS Appl. Mater. Interfaces*, 2020, **12**, 38124–38131.
90 A. Afzalinia and M. Mirzaee, *ACS Appl. Mater. Interfaces*, 2020, **12**, 16076–16087.
91 S. Wu, Y. Lin, J. Liu, W. Shi, G. Yang and P. Cheng, *Adv. Funct. Mater.*, 2018, **28**, 1707169.
92 K. Shi, Z. Yang, L. Dong and B. Yu, *Sens. Actuators, B*, 2018, **266**, 263–269.
93 X. Li, S. Zhou, S. Lu, D. Tu, W. Zheng, Y. Liu, R. Li and X. Chen, *ACS Appl. Mater. Interfaces*, 2019, **11**, 43989–43995.
94 X. Dai, J.-N. Hao, J. Gu and Y. Li, *ACS Appl. Bio Mater.*, 2020, **3**, 3792–3799.
95 J. N. Hao, D. Niu, J. Gu, S. Lin, Y. Li and J. Shi, *Adv. Mater.*, 2020, **32**, 2000791.
96 D. Yue, Y. Huang, L. Zhang, K. Jiang, X. Zhang, Y. Cui, Y. Yu and G. Qian, *J. Mater. Chem. C*, 2018, **6**, 2054–2059.
97 H. Weng and B. Yan, *Sens. Actuators, B*, 2017, **253**, 1006–1011.
98 A. F. Yang, S. L. Hou, Y. Shi, G. L. Yang, D. B. Qin and B. Zhao, *Inorg. Chem.*, 2019, **58**, 6356–6362.
99 Y. Zhao, M.-Y. Wan, J.-P. Bai, H. Zeng, W. Lu and D. Li, *J. Mater. Chem. A*, 2019, **7**, 11127–11133.
100 J. Xiao, L. Song, M. Liu, X. Wang and Z. Liu, *Inorg. Chem.*, 2020, **59**, 6390–6397.
101 T. Y. Luo, P. Das, D. L. White, C. Liu, A. Star and N. L. Rosi, *J. Am. Chem. Soc.*, 2020, **142**, 2897–2904.
102 J. M. Wang, X. Lian and B. Yan, *Inorg. Chem.*, 2019, **58**, 9956–9963.
103 M. C. Heffern, L. M. Matosziuk and T. J. Meade, *Chem. Rev.*, 2014, **114**, 4496–4539.
104 X. Z. Li, L. P. Zhou, L. L. Yan, D. Q. Yuan, C. S. Lin and Q. F. Sun, *J. Am. Chem. Soc.*, 2017, **139**, 8237–8244.
105 Q. Ma, M. Zhang, X. Xu, K. Meng, C. Yao, Y. Zhao, J. Sun, Y. Du and D. Yang, *ACS Appl. Mater. Interfaces*, 2019, **11**, 47404–47412.
106 J. D. Routledge, X. Zhang, M. Connolly, M. Tropiano, O. A. Blackburn, A. M. Kenwright, P. D. Beer, S. Aldridge and S. Faulkner, *Angew. Chem., Int. Ed.*, 2017, **56**, 7783–7786.
107 H. Ma, K. Chen, B. Song, Z. Tang, Y. Huang, T. Zhang, H. Wang, W. Sun and J. Yuan, *Biosens. Bioelectron.*, 2020, **168**, 112560.
108 J. Guo, C. Mingoes, X. Qiu and N. Hildebrandt, *Anal. Chem.*, 2019, **91**, 3101–3109.
109 B. Brennecke, Q. Wang, Q. Zhang, H. Y. Hu and M. Nazare, *Angew. Chem., Int. Ed.*, 2020, **59**, 8512–8516.
110 S. Zhou, D. Tu, Y. Liu, W. You, Y. Zhang, W. Zheng and X. Chen, *Adv. Sci.*, 2021, **8**, 2002657.
111 Q. X. Wang, S. F. Xue, Z. H. Chen, S. H. Ma, S. Zhang, G. Shi and M. Zhang, *Biosens. Bioelectron.*, 2017, **94**, 388–393.
112 S. Qu, N. Song, G. Xu and Q. Jia, *Sens. Actuators, B*, 2019, **290**, 9–14.

113 M. Donmez, H. A. Oktem and M. D. Yilmaz, *Carbohydr. Polym.*, 2018, **180**, 226–230.
114 K. Luan, R. Meng, C. Shan, J. Cao, J. Jia, W. Liu and Y. Tang, *Anal. Chem.*, 2018, **90**, 3600–3607.
115 P. Su, X. Wang, T. Wang, X. Feng, M. Zhang, L. Liang, J. Cao, W. Liu and Y. Tang, *Talanta*, 2021, **225**, 122063.
116 R. C. Knighton, L. K. Soro, A. Lecointre, G. Pilet, A. Fateeva, L. Pontille, L. Frances-Soriano, N. Hildebrandt and L. J. Charbonniere, *Chem. Commun.*, 2021, **57**, 53–56.
117 A. Nonat, S. Bahamyirou, A. Lecointre, F. Przybilla, Y. Mely, C. Platas-Iglesias, F. Camerel, O. Jeannin and L. J. Charbonniere, *J. Am. Chem. Soc.*, 2019, **141**, 1568–1576.